Biology Faculty Articles   Department of Biological Sciences

6-7-2023

Patrolling the Border: Billfish Exploit the Hypoxic Boundary Created by the World's Largest Oxygen Minimum Zone

Ryan Logan
Nova Southeastern University, rklogn@gmail.com

Jeremy J. Vaudo
Nova Southeastern University, jvaudo@nova.edu

Brad Wetherbee
Nova Southeastern University, bwetherb@nova.edu

Mahmood Shivji
Nova Southeastern University, mahmood@nova.edu

Follow this and additional works at: https://nsuworks.nova.edu/cnso_bio_facarticles

Part of the Biology Commons

RESEARCH ARTICLE

Patrolling the border: Billfish exploit the hypoxic boundary created by the world's largest oxygen minimum zone

Ryan K. Logan[1] | Jeremy J. Vaudo[1] | Bradley M. Wetherbee[1,2] | Mahmood S. Shivji[1]

[1]Guy Harvey Research Institute, Halmos College of Arts & Sciences, Nova Southeastern University, Dania Beach, Florida, USA

[2]Department of Biological Sciences, University of Rhode Island, Kingston, Rhode Island, USA

Correspondence
Ryan K. Logan
Email: rklogn@gmail.com

Abstract

1. Pelagic predators must contend with low prey densities that are irregularly distributed and dynamic in space and time. Based on satellite imagery and telemetry data, many pelagic predators will concentrate horizontal movements on ephemeral surface fronts—gradients between water masses—because of enhanced local productivity and increased forage fish densities.

2. Vertical fronts (e.g. thermoclines, oxyclines) can be spatially and temporally persistent, and aggregate lower trophic level and diel vertically migrating organisms due to sharp changes in temperature, water density or available oxygen. Thus, vertical fronts represent a stable and potentially energy rich habitat feature for diving pelagic predators but remain little explored in their capacity to enhance foraging opportunities.

3. Here, we use a novel suite of high-resolution biologging data, including in situ derived oxygen saturation and video, to document how two top predators in the pelagic ecosystem exploit the vertical fronts created by the oxygen minimum zone of the eastern tropical Pacific.

4. Prey search behaviour was dependent on dive shape, and significantly increased near the thermocline and hypoxic boundary for blue marlin *Makaira nigricans* and sailfish *Istiophorus platypterus*, respectively. Further, we identify a behaviour not yet reported for pelagic predators, whereby the predator repeatedly dives below the thermocline and hypoxic boundary (and by extension, below the prey). We hypothesize this behaviour is used to ambush prey concentrated at the boundaries from below.

5. We describe how habitat fronts created by low oxygen environments can influence pelagic ecosystems, which will become increasingly important to understand in the context of global change and expanding oxygen minimum zones. We anticipate that our findings are shared among many pelagic predators where strong vertical fronts occur, and additional high-resolution tagging is warranted to confirm this.

KEYWORDS
biologging, hunting behaviour, marlin, oceanic front, oxygen minimum zone, pelagic predator, sailfish

1 | INTRODUCTION

Ecological theory predicts that when prey are sparse and patchily distributed, predators should move, forage and engage in activity patterns that maximize energetic gain while minimizing energetic loss (Pyke et al., 1977; Stephens & Krebs, 1986). Because foraging success is positively related to resource density (Mysterud & Ims, 1998), predators should forage (e.g. elevate activity and search behaviour) in habitats with high resource density (McMahon & Matter, 2006). In the pelagic environment, oceanic fronts are one such location. Oceanic fronts—strong gradients in abiotic factor(s) (e.g. temperature) caused by the convergence of water masses with different properties—create hotspots of biogeochemical cycling and aggregate low trophic level organisms (Woodson & Litvin, 2015).

Because oceanic fronts influence prey distribution, studies of highly mobile marine predators often focus on movements and distribution in relation to fronts (Arostegui et al., 2022; Sequeira et al., 2018). While this information provides valuable insight of when and where predators encounter prey and use frontal habitat, they often lack the resolution necessary to describe how the fronts are exploited (but see Arostegui et al., 2022). Further, because satellite imagery of oceanic conditions is limited to surface waters, such studies of pelagic predator movements in relation to fronts are biased towards horizontal movements and surface fronts. Yet, marine predators live in a three-dimensional habitat and must respond to variable prey density both horizontally and vertically to maximize energy acquisition.

Vertical fronts such as thermoclines, oxyclines and pycnoclines can be spatially and temporally persistent in oceanic basins, concentrate basal food resources and act as barriers to many prey items seeking refuge during daylight hours (Derenbach et al., 1979; Fortune et al., 2020). For example, two species of manta ray were observed to concentrate feeding behaviour on high-density zooplankton prey aggregated at the thermocline (Stewart et al., 2019). Similarly, little penguin *Eudyptula minor* prey encounter rates were positively correlated with well-stratified waters, as prey were less dispersed in the available habitat and concentrated at the thermocline (Ropert-Coudert et al., 2009). As such, vertical fronts have the potential to be rich in energy, but our knowledge of how top pelagic predators respond to and use these fronts remains limited.

High-resolution acceleration biologging can fill the knowledge gap of how top pelagic predators may exploit vertical fronts because it allows for the examination of animal behaviours not under direct observation (Watanabe & Takahashi, 2013; Wilson et al., 2008; Yoda et al., 1999). By incorporating additional sensors such as tri-axial magnetometers and gyroscopes, the animal's heading and turning can be directly quantified (Andrzejaczek et al., 2019; Williams, Holton, et al., 2017). Finally, by combining these animal movement sensors with abiotic variables such as depth, temperature and in situ oxygen concentration (Coffey & Holland, 2015), a more complete picture of animal movements and search behaviour in relation to vertical fronts can be attained.

The Eastern Tropical Pacific (ETP) features a narrow (~25–50 m; spatially and temporally variable), productive surface layer of uniform temperature and oxygen saturation, followed by a shallow and sharp thermocline (Fiedler & Lavín, 2017). Coexistent with the thermocline is the upper boundary of the oxygen minimum layer, beyond which lies the world's largest naturally occurring oxygen minimum zone (OMZ; Gallo & Levin, 2016). Because cold temperatures and hypoxic conditions limit the vertical and horizontal distribution of many fishes, predators and prey alike of the ETP are confined to surface waters above the OMZ, known as hypoxia-based habitat compression (Brill et al., 1998; Prince et al., 2010; Stramma et al., 2012). During daylight hours, as prey species attempt to escape predation pressure by moving into lower-lit waters, prey density increases around this hypoxic boundary (Bertrand et al., 2006, 2010; Bianchi et al., 2013). As such, the ETP provides an opportune environment to study the fine-scale vertical habitat use and hunting behaviour of pelagic predators in relation to vertical fronts. Information of predator habitat use and hunting behaviour in relation to hypoxic boundaries is of economic and ecological interest as global climate change intensifies. Increasing global sea surface temperatures will serve to reduce global ocean oxygen content and strengthen upper ocean stratification, which will increase productivity in surface waters, fueling increased oxygen demand while simultaneously reducing oxygen supply to greater depths (Keeling et al., 2010). Under these scenarios, oxygen minimum zones will become shallower and increase in size, affecting new regions and ecosystems (Laffoley & Baxter, 2019). Thus, predator foraging behaviour in the ETP could provide insight into future vertical habitat use of pelagic predators worldwide.

Here, we use a novel combination of high-resolution biologging and animal-borne video of blue marlin *Makaira nigricans* and sailfish *Istiophorus platypterus* to examine the relationship between their vertical and horizontal movements in a vertically compressed habitat. Additionally, we determine how these highly migratory predators may exploit the vertical fronts created by an oxygen minimum zone to increase foraging opportunities.

2 | MATERIALS AND METHODS

Blue marlin and sailfish were caught using rod-and-reel on trolling lures or natural live bait off the Pacific coast of southeast Panama from September to November 2019. Each fish was brought alongside the vessel and a custom-designed biologging tag package was affixed to the dorsal musculature with two umbrella-style anchors using a custom-made tag applicator. Once both anchors were securely imbedded in the muscle, the tag was firmly cinched against the fish's body using two galvanic timed releases and a cable tie. Fish weight was estimated by an experienced captain.

The biologging tag package consisted of an inertial measurement unit (IMU; OpenTag 3.0; Loggerhead Instruments), video camera (DVL 2000M130; Little Leonardo) and a Smart Position and Temperature tag (SPOT-363A; Wildlife Computers) for package

recovery (Figure S1). The IMU comprised a triaxial accelerometer, magnetometer, and gyroscope recording at 100 Hz, depth, temperature, and a small turbine-based fluid speed sensor recording at 1 Hz. Two IMUs were equipped with a small (12 mm diameter × 20 mm long) oxygen sensor (Micro Probe; OxyGuard) that recorded in situ dissolved oxygen (% saturation) of the water at 1 Hz. Because not all IMUs contained an oxygen sensor, four blue marlin and four sailfish did not have accompanying oxygen data. Therefore, we calculated mean in situ % dissolved oxygen and depth profiles at 0.5-m-depth intervals from each deployment with an oxygen sensor, and assigned resulting oxygen values to the corresponding depths of fish without oxygen readings. For further description on data products, methodology and biologging tag package see Logan et al. (2022). Data used in the current study are from the tag deployments described in Logan et al. (2022) after excising the unique time prior to recovery for each fish (see Table 1; Logan et al., 2022). All fish were tagged under permit from the Ministerio de Ambiente, República de Panamá (SE/A-64-19), and procedures approved by Nova Southeastern University's Institutional Animal Care and Use Committee (2019.04.MS1).

2.1 | Diel habitat use

Using animal-borne temperature and oxygen sensors, mean overall depth profiles were generated for each variable at 0.5 m depth intervals by pooling all individuals' depth, temperature, and oxygen data. The thermocline was calculated as the shallowest depth at which the water temperature differs from sea surface temperature by 0.8°C (Delta *T*; Fiedler, 2010). As there is no universal definition of what percent oxygen saturation constitutes an oxycline, we consider the oxycline to be the shallowest depth at which percent oxygen saturation begins to decline more drastically with depth than in the water above, which in our study was determined to be 90% of that at the surface (100% saturation). Similarly, because there is no single oxygen concentration that defines a universal level of hypoxic stress for all marine organisms (Seibel, 2011), we adopt the dissolved oxygen level of ≤3.5 mL L^{-1} threshold identified to induce stress in tropical pelagic fishes (Bushnell & Brill, 1991; Prince & Goodyear, 2006) as the hypoxic boundary for blue marlin and sailfish (which occurs at ~60%–65% O$_2$ saturation at 19–25°C). All observations were categorically assigned to either day or night periods.

2.2 | Dive shape

Variable dive shapes across diving marine taxa have been linked to a variety of behaviours (Braun et al., 2022; Carter et al., 2016). Because blue marlin and sailfish dives did not all follow the same pattern, dive profiles were categorized based on their similarity of shape via cluster analysis. Here, we define a dive as a vertical excursion to a minimum of 10 m and lasting at least 20 s. Because gill breathing animals do not need to come to the surface, a depth threshold was necessary to isolate movements clearly directed away from the surface.

Depths from each qualifying dive were either downsampled or interpolated (depending on duration of the dive) so that each dive consisted of 50 depths equally spaced across the dive duration. Depths were then scaled so the start and end of each dive were equal to zero and the maximum dive depth equal to one, thus standardizing dive depths and lengths (Schreer et al., 1998). Using the 'FACTOEXTRA' package in R (Kassambara & Mundt, 2017), we conducted hybrid hierarchical *k*-means clustering on the standardized dive profiles. The optimal number of dive shapes (i.e. clusters) was determined using an ensemble approach in which the elbow method, the silhouette method and the gap statistic method (Tibshirani et al., 2001) were compared and evaluated for biological realism (i.e. compared to previous known dive shapes of pelagic predators and eliminated clusters with few observations).

To determine how fish behaviour varied among dive shapes, depth, maximum depth, temperature, % oxygen saturation, descent rate, ascent rate, dive duration, bottom time, overall dynamic body accelerations (ODBA), maximum ODBA, and tailbeat frequency (TBF) were summarized for each dive shape. OBDA and TBF were calculated by summing the absolute value of the dynamic acceleration from all three axes (Wilson et al., 2006), and using a continuous wavelet transformation in Igor Pro v. 8.0.4.2 (Wavemetrics, Inc.) with the Ethographer extension (Sakamoto et al., 2009), respectively. Dive characteristics of each dive shape were compared within species using a multivariate analysis of variance (MANOVA). Where significant differences were identified, pairwise comparisons were examined using a non-parametric Games-Howell post-hoc test.

2.3 | Path tortuosity and video

To investigate relationships between path tortuosity (a proxy for prey searching), vertical habitat characteristics and dive shape, general additive mixed models (GAMMs) were built in R using the MGCV package (Wood, 2015). First, a 3-s box smoothing window was applied to the heading data to filter out movements of the fish caused by the tailbeats. Filtered heading data (0–360°) were resampled to a 1-s frequency and used to calculate the turning angles of each individual by calculating the absolute difference in angle between consecutive observations. Then, turning angles were summed across 1-min periods, creating a continuous measure of path tortuosity. Because habitat characteristics of depth, temperature, and oxygen were correlated (Pearson correlation coefficients: 0.65–0.7), a principal component analysis (PCA) was conducted to reduce dimensionality and retain the greatest amount of information about the correlated variables in space. Principal components with greater than 10% of variance explained were included as candidate predictor variables in GAMMs. Tortuosity was the response variable, and habitat principal components and dive shape were explanatory variables. The model was run using a Gaussian response distribution and identity link (determined to be the best fitting distribution via AIC), and we used the corAR1 function (first order autocorrelation structure;

TABLE 1 Summary details of tagged blue marlin (BUM) and sailfish (SFA). Time retained indicates the amount of time used for analyses in this study, after removal of the unique recovery period for each fish from Logan et al. (2022).

Fish ID	Deployment date	Estimated mass (kg)	Total tag attachment duration (h)	Time retained (h)	Depth (m)		Water temperature (°C)		% oxygen saturation	
					Mean ± SD	Range	Mean ± SD	Range	Mean ± SD	Range
BUM1	2019-09-22 12:00	160	14.8	7.1	3.4±3.7	2-35.7	27.5±0.1	26.5-27.7	87.9±5.8	69-98.8
BUM2	2019-09-24 12:40	205	34.0	25.3	8.7±9.4	0.1-52.7	27.7±0.7	19.1-28.7	93.1±7.6	10-100
BUM3	2019-10-03 12:29	115	35.9	25.6	21.7±10.2	4.6-43.3	27±1	20.7-27.6	87.8±10.8	18.8-95.1
BUM4	2019-10-03 13:41	90	36.4	29.4	5.5±9	0.7-40.6	28.1±0.6	25.6-29.9	95.8±4	60.1-99
BUM5	2019-10-05 14:33	90	35.9	18.6	6±8.3	0.2-41.3	27.1±0.2	24.9-28.3	96.1±2	57.4-98.5
BUM6	2019-10-09 14:15	115	32.1	21.7	6.9±9.2	1.6-51.9	27.6±0.5	21.9-28.7	90.7±5.3	30.8-98.6
BUM7	2019-10-21 11:27	115	32.7	24.6	3.1±6.7	0.1-51.6	27.4±0.5	22.5-27.8	95.4±6.1	30.8-99
BUM8	2019-10-25 14:35	180	67.0	58.0	5.6±4.7	0.3-55.4	27.5±0.4	22.7-27.9	94.2±5.4	22.9-100
BUM9	2019-10-30 12:03	70	70.5	59.1	2.6±6.5	0.1-52.3	27.6±0.3	23.7-28.1	97.1±3.5	21.6-100
SFA1	2019-09-19 10:38	50	16.8	11	5.1±5.8	0.1-55.2	27.4±0.8	19.9-27.8	92.9±7.2	20.8-99
SFA2	2019-09-23 12:00	30	13.4	8.8	1.5±0.3	0.1-7.5	27.8±0.01	27.7-27.9	98.5±1.3	92-100
SFA3	2019-10-09 11:41	25	33.5	28.5	8±14.5	0.2-67.9	27.4±1.3	21-28.9	84.4±15	7.5-99.7
SFA4	2019-10-14 11:20	45	36.8	32.7	9.2±10.8	0.2-46.9	27.4±0.6	22.8-28.2	91.1±7.9	24-100
SFA5	2019-10-15 13:17	45	60.3	55.0	7.1±9.8	0.02-63.8	27.7±1	19.9-28.4	90.2±10.1	9.4-99
SFA6	2019-10-18 09:53	45	67.2	62.4	7.3±11.5	0.01-62.4	27.4±0.8	20.9-28.7	94.4±12.1	6.4-100
SFA7	2019-10-27 11:13	35	38.7	33.4	4.6±6.4	0-46.5	27.8±0.1	25.5-28.2	94.3±2.8	46.8-99
SFA8	2019-10-31 10:13	45	18.9	13.3	4±5	1.6-37.5	28.1±0.1	27.1-28.3	92.8±2.1	62.2-97.9
SFA9[a]	2019-11-04 14:07	35	6.1	NA	6±6.5	0.6-33.9	28.5±0.5	27.3-29.1	94.2±1.7	82.3-100

[a]Eliminated from analyses due to short tag attachment duration.

adds a variance–covariance matrix accounting for the correlation of observations) within each individual to account for temporal auto-correlation in the data, with individual included as a random intercept (Pinheiro & Bates, 2006; Zuur et al., 2009). Model fit was assessed by examining residual diagnostic plots, and Akaike's information criterion (AIC) was used to assess model performance against an intercept only model, with improved model fit indicated by a ∆AIC value >2. Tortuosity was log-transformed prior to model fitting. Finally, the onboard video camera was used to ground-truth periods of high tortuosity, and interaction with con- and herterospecifics.

3 | RESULTS

Nine blue marlin and nine sailfish were caught and tagged between 2019-09-19 and 2019-11-04 (Table 1). Mean estimated mass was 125 ± 45 kg for blue marlin, and 40 ± 10 kg for sailfish, which are representative of the size classes of the majority of fish caught in this region for each species (R. White, *pers. comm*). Tags were attached for 36.2 ± 18.7 h (mean ± SD), recording 81 and 75 h of video footage for blue marlin and sailfish, respectively. After censoring the unique time it took each individual to recover post-release (Table 1; see Logan et al., 2022), 271 and 245 h of IMU data were retained for analysis for blue marlin and sailfish, respectively.

3.1 | Diel habitat use

After combining water column profiles of depth, temperature and oxygen across all fish, the calculated thermocline (Delta T 0.8°C) occurred at a depth of 31.3 ± 3.8 m, the oxycline (90% oxygen saturation) at 27.7 ± 2.7 m and the hypoxic boundary (60%–65% oxygen saturation) at 39.8 ± 2 m (Figure 1a,d).

In general, blue marlin and sailfish spent most of their time in the upper mixed layer of the water column, though there were differences in depth use between day and night for each species. During the day, blue marlin mean depth was 5.3 ± 8.4 m with a maximum depth of 55 m (blue marlin 8). Blue marlin spent 88% of the day at depths of 0–10 m, and 96% of their time shallower than 30 m, in water temperatures of 27–28°C (90% of time), and at oxygen saturation levels of 90%–100% (90% of time; Figure 1b,c). During daylight hours, blue marlin descended below the thermocline and oxycline 3% and 5% of their time, respectively, with 2.8% of time spent around the thermocline (27–31 m; Figure 2b). Less than 1% of their time was spent below the hypoxic boundary. At night, blue marlin average depth was 4.7 ± 6.6 m (maximum depth 51.9 m) with 90% of time spent between 0 and 10 m, 95% of time at water temperature between 27 and 28°C and 90% of time at oxygen saturation levels of 90%–100% (Figure 1). Diving at night was less common, as blue marlin descended below the thermocline 2% of the time, below the oxycline 3% of the time, and below the hypoxic boundary <0.5% of the time. When blue marlin descended below the mixed layer, they

typically experienced Delta T of <2°C, and Delta O_2 of <10% O_2 saturation (Figure 2c,d). Maximum Delta T and maximum Delta O_2 experienced were 8.5°C and 85% O_2 saturation, respectively.

Sailfish were more vertically active than blue marlin (i.e. performed more dives), yet also spent most time within the mixed layer. During daylight hours, sailfish mean depth was 7.7 ± 12.4 m, with a maximum depth of 67.9 m (sailfish 3). Sailfish spent the majority (84%) of their daylight hours from 0 to 10 m depth, at water temperatures of 27–28°C (85%) and at oxygen saturation levels of 90%–100% (76%; Figure 1e,f). During daylight hours, sailfish descended below the thermocline 10% of the time, below the oxycline 11% of the time and below the hypoxic boundary 6% of the time, but showed an increase in proportion of time spent near the hypoxic boundary (~38 m; Figure 2b). Sailfish average depth at night was 6.1 ± 8.5 m (maximum of 60.1 m), with 87% of time spent within 0–10 m, 94% of time in 27–28°C water and 81% of time at oxygen saturation levels of 90%–100%. At night, sailfish descended below the thermocline 3% of the time, below the oxycline 5% of the time and below the hypoxic boundary <1% of the time. Maximum Delta T and Delta O_2 experienced by sailfish were 7.8°C and 87% O_2, respectively (Figure 2c,d).

3.2 | Dive shape

A total of 176 blue marlin dives and 231 sailfish dives were classified. Upon visual inspection of the different dive shapes and previous knowledge of the diving behaviour of pelagic fishes, the optimal number of dive shapes (clusters) for blue marlin and sailfish were selected as three and five, respectively (see Figure S2). Both species displayed U, V, and W dive shapes, but sailfish also exhibited long-ascent (LA) and long-descent (LD) dive shapes (Figure 3). U dives featured a descent and ascent of similar duration separated by an extended bottom phase, while V dives lack the extended bottom phase. LD dives had a descent phase that lasted most of the dive, a limited bottom phase, and short ascent. LA dives had a short descent phase, a limited bottom phase, and an ascent that lasted most of the dive. W dives were characterized by a rapid descent, followed by one or more small-scale vertical movements within the bottom phase of the dive, and a rapid ascent (Figure 3; Table 2).

Environmental and behavioural characteristics among dive shapes differed within blue marlin ($F_{(22,312)} = 10.34$, $p < 0.001$) and sailfish ($F_{(44,856)} = 7.78$, $p < 0.001$). U dives were the most common dive shape for blue marlin (51%) and sailfish (34%), followed by V dives in blue marlin (30%) and LA dives in sailfish (32%). For blue marlin, dives with an extended bottom phase (U and W) were deeper, during which fish experienced lower mean temperatures and oxygen concentrations than V dives (Table 2). Dive duration and bottom time were the longest during W dives, but neither ODBA, maximum ODBA nor TBF differed among dive shapes for blue marlin or sailfish (Table 2). Sailfish displayed a greater variety of dive shapes than blue marlin, but in both species U and W dives were longer, deeper, colder and to lower oxygen saturation than other dive shapes (Table 2). Sailfish W dives had the deepest average and maximum depths of
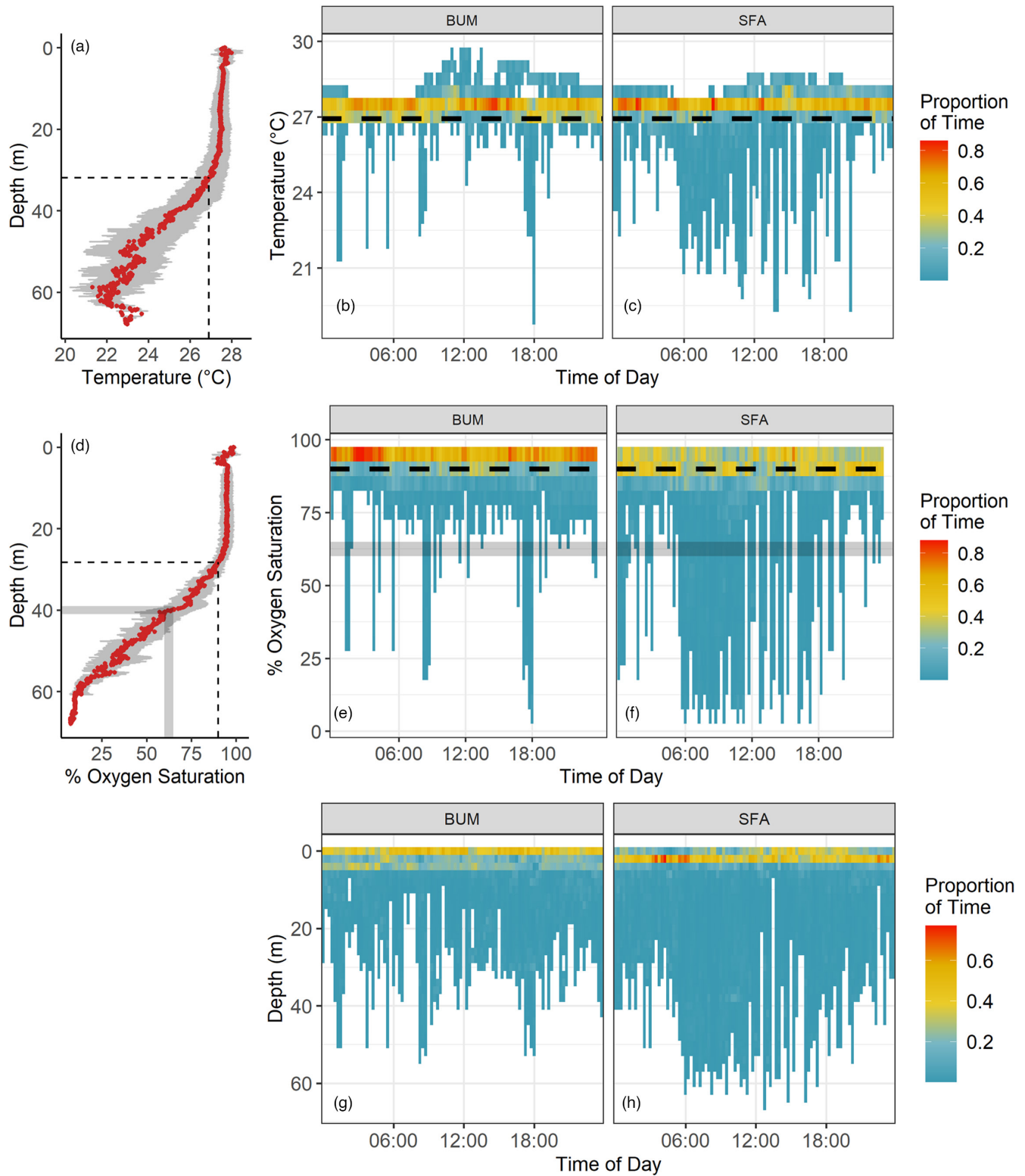
FIGURE 1 Vertical habitat characteristics and diel patterns in temperature, dissolved oxygen and depth use. (a) Mean water column profiles of depth and temperature and (d) depth and % oxygen saturation measured from tagged fish (red) with grey shading indicating ±1 SD across all tags. (b, c) indicate mean time spent at temperature (0.5° bins), (e, f) % oxygen saturation (5% bins), and (g, h) depth (2 m bins) for blue marlin and sailfish. Dashed lines indicate the thermocline temperature in a–c and the oxycline % oxygen concentration in d–f. Shaded regions in d–f indicate the estimated % oxygen concentration of the $3.5\,mL\,L^{-1}$ hypoxic boundary threshold. BUM, blue marlin; SFA, sailfish.
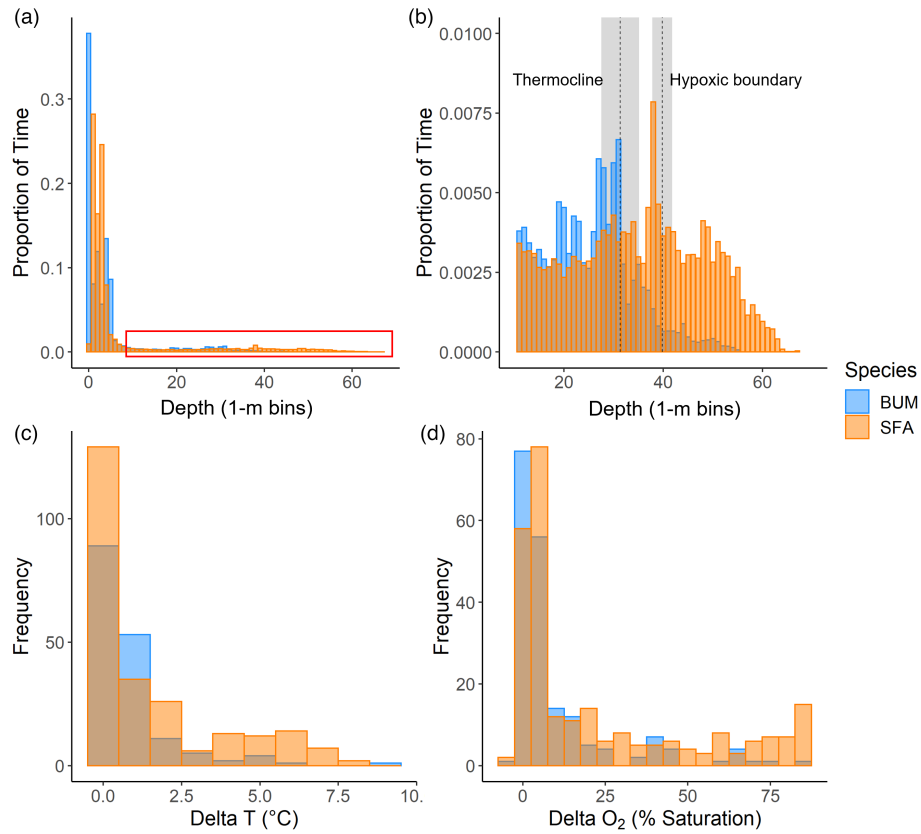
FIGURE 2 Vertical daytime distribution and minimum temperatures and % oxygen saturation experienced during dives by blue marlin (BUM) and sailfish (SFA). Percent time spent at 1-m depth intervals during daytime hours in (a), with (b) zoomed in on the tail of (a; red outline) to highlight increases near vertical habitat fronts. In (b), vertical dotted lines and grey shading indicate the mean ± 1 SD depth of the thermocline and hypoxic boundary as determined in situ by biologging tags (see methods). (c) Minimum temperatures experienced relative to the mixed layer (Delta T; °C) and (d) % oxygen saturation relative to the mixed layer (Delta %O_2 saturation) during dives.
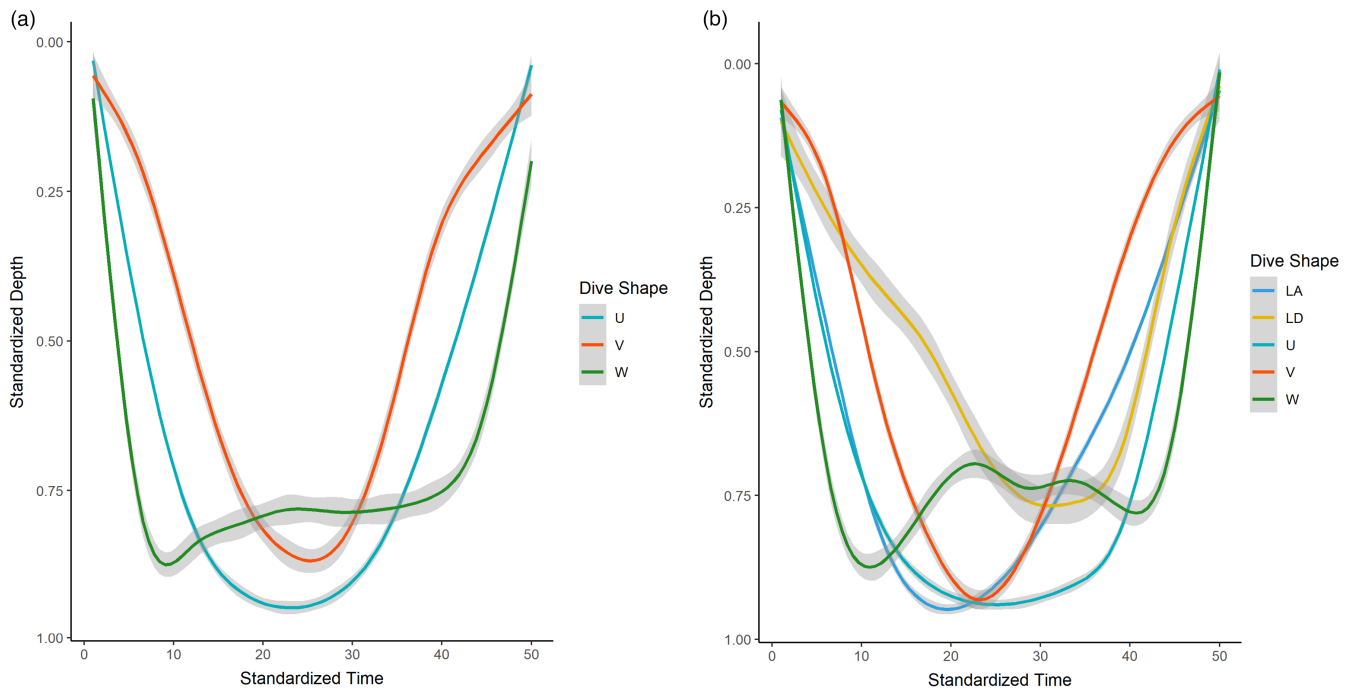
FIGURE 3 Smoothed dive shapes (solid lines) determined by hierarchical clustering of standardized dive profiles for blue marlin (a) and sailfish (b).

TABLE 2 Summary statistics (mean±SD) for the dive shapes identified via hybrid hierarchical k-means clustering for blue marlin and sailfish. Statistical results are from a multivariate analysis of variance (MANOVA) of dive-shape characteristics. Values followed by the same letter are not significantly different at the 0.05 significance level, using a Games-Howell post-hoc test for pairwise comparisons.

Dive Shape	n	MANOVA F (df)	P	Mean Depth	Max Depth	Temperature	% Oxygen Saturation	Descent Rate	Ascent Rate	Duration (min)	Bottom Time (min)	ODBA	Max ODBA	TBF
Blue marlin														
U	89	(22,312) 10.34	<0.001	17.8±6.1 a	26±10.1 a	27.3±0.6 a	93±7 a	0.13±0.05 a	0.11±0.03 a	10.9±4.7 a	5.2±2.5 a	0.061±0.007 a	0.22±0.24 a	0.51±0.07 a
V	52			12.1±4.8 b	21.8±10.8 b	27.6±0.3 b	95±3 b	0.22±0.21 b	0.17±0.13 b	5.5±4 b	1.6±1.3 b	0.078±0.04 a	0.38±0.67 a	0.57±0.2 a
W	35			18.9±7.9 a	26±11.5 b	27.2±0.6 a,b	92±8 a	0.15±0.06 a,b	0.1±0.04 a	22.7±15.5 c	9.5±7.5 c	0.064±0.03 a	0.31±0.32 a	0.53±0.14 a
Sailfish														
LA	73	(44,856) 7.78	<0.001	17.2±8 a	25.5±14.1 a	27.3±0.9 a	89±10 a	0.17±0.09 a	0.13±0.07 a	7.2±4.6 a	2.9±1.8 a	0.046±0.01 a	0.22±0.27 a	0.64±0.06 a
LD	18			17.9±6.9 a	34.1±14.5 a,b	27.3±0.6 a	89±9 a	0.2±0.09 a	0.45±0.6 a	7.9±4.8 a,b	1.7±1.8 a,b	0.059±0.03 a	0.29±0.25 a	0.64±0.12 a
U	78			25.5±9.1 b	35.3±13.5 b	26.7±1.3 b	82±15 a,b	0.16±0.09 a	0.2±0.4 a,b	12.3±5.2 c	6.9±3.2 c	0.05±0.03 a	0.41±1.4 a	0.62±0.09 a
V	35			15.2±6.9 a	26.4±13.2 a	27.3±0.7 a	90±10 a	0.24±0.13 a,b	0.23±0.15 a	4.5±3.9 a,b	1.3±0.9 a,b	0.057±0.02 a,b	0.27±0.3 a	0.69±0.1 a,b
W	27			30.9±10 b	45.3±15.9 b,c	26.1±1.4 b	74±16 b	0.19±0.05 a	0.2±0.08 a	18.7±10.1 d	6.9±4.8 c	0.056±0.01 a,b	0.27±0.13 a	0.66±0.07 a,b

any dive shape for either species, and were also the longest duration dives performed by sailfish (Table 2).

## 3.3 | Path tortuosity and video

Physical water column characteristics (temperature, % oxygen saturation, depth) and dive shape were examined to determine their influence on fish path tortuosity. Because blue marlin and sailfish are visual predators, only daytime dives were used. Path tortuosity was different among dive shapes for both species (blue marlin Kruskal–Wallis $\chi^2 = 25.3$, df = 2, $p < 0.001$; sailfish $\chi^2 = 25.8$, df = 4, $p < 0.001$). Pairwise comparisons revealed blue marlin dive tortuosity was greatest for W dives, followed by U dives and V dives (Table S1) and sailfish dive tortuosity was greatest for W and U dives, followed by LA dives (Table S2).

The first principal component (PC1) of depth, ambient water temperature and ambient % oxygen saturation explained 79% of variance, and the second principal component (PC2) explained 11.5% of variance so both were included in candidate GAMMs. Large and similar loadings on PC1 for depth (0.57), temperature (−0.57) and oxygen (−0.59) indicate that each variable was an important contributor to PC1, and that increasing values of PC1 indicate deep, cold and oxygen poor water. Loadings were similarly large on PC2 for depth (−0.71) and temperature (−0.7), but not oxygen (−0.001), such that increases in PC2 are indicative of shallower but cold water.

Blue marlin path tortuosity was best described by the model that included the interaction of water temperature and dive shape, which explained 51.8% of deviance of path tortuosity (Table S3). Blue marlin exhibited increased tortuosity at low temperatures during U and W dives; tortuosity increased during the coldest portion (below ~22°C) in U dives (Figure 4a) and was elevated in W dives starting at the thermocline (~27°C) and extending into colder water (Figure 4b). Tortuosity was not impacted by temperature during V dives.

The best fitting model for sailfish path tortuosity included PC1, PC2 and dive shape, explaining 58.9% of deviance (Table S4). Path tortuosity was low at the lowest PC1 values, corresponding to movements near the surface (Figure 5a,c). However, sailfish path tortuosity increased at and adjacent to the hypoxic boundary. For example, sailfish tortuosity increased at PC1 values ranging from ~3.5 to 11 (Figure 5a), corresponding to a median depth of 39 m (IQR 36–45 m), temperature of 25.4°C (IQR 24.2–26.2°C) and % oxygen saturation of 65% (IQR 50%–76%). Similarly, sailfish tortuosity increased along PC2 values of 2–3 (Figure 5b), corresponding to a similar median depth of 41 m (IQR 2–51 m), temperature of 22.4°C (IQR 21.6–25.3°C) and oxygen saturation of 48% (IQR 29%–90%).

In total, we obtained 156 h of video footage (81 blue marlin and 75 h sailfish), which captured interactions with con- and heterospecifics. For example, video enabled identification of high activity periods, or when other animals were present in the field of view of the animal carrying the tag package. Across all sailfish tag deployments, video footage showed at least one other sailfish in the frame on 40 separate occasions, with a maximum of three other sailfish in frame
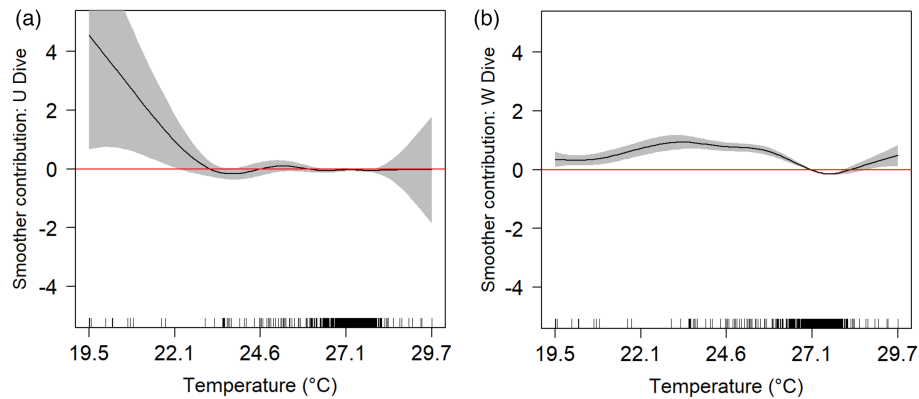
FIGURE 4 Response curves from the best-fit general additive mixed model (black solid line) for blue marlin tortuosity by dive shape. Shaded areas represent 95% confidence limits and positive values on *y*-axis (above red line) indicate increased tortuosity by blue marlin. Ticks on *x*-axis denote values for which there are data. V-dives are omitted because there was no relationship.
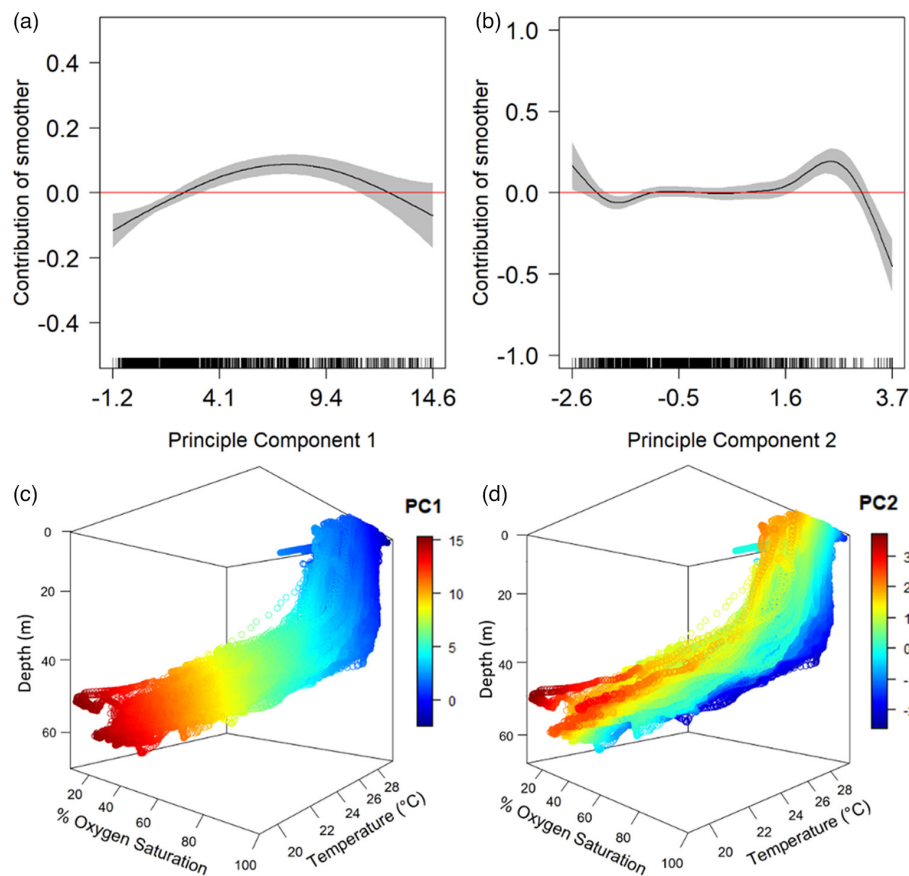

FIGURE 5 (a, b) Response curves from the best-fit general additive mixed model (black solid line) for sailfish path tortuosity. Shaded areas represent 95% confidence; positive values on *y*-axis (above red line) indicate increased tortuosity by sailfish. (c, d) Principal component scores (values given by colour scale) as distributed in coordinates of co-located depth, water temperature, and dissolved oxygen saturation.

at one time (although the video would suggest there were more than three individuals present; Video S1). In the majority of sightings, sailfish were in very close proximity (~1–2 BL) to the tagged fish (Video S2). During sailfish tag deployments, other sailfish were encountered at the surface and at depth, indicating behaviours expressed by the tagged individual were shared among untagged fish (Figure 6). Smaller, potential prey fishes were observed occasionally

but were not pursued by tagged sailfish (Figure S3). No con- or heterospecific interaction was observed in any blue marlin footage. Furthermore, video footage showed very little visible light past ~50 m during daylight hours (Figure 6).

Repetitive diving below the hypoxic boundary during W dives was common among sailfish. This behaviour was characterized by rapid descents to below the hypoxic boundary where the fish would
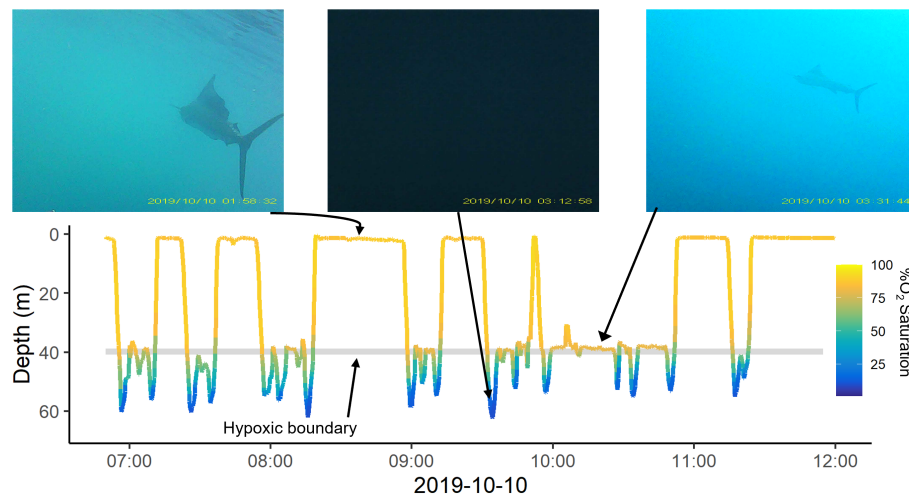
FIGURE 6 Excerpt of diving behaviour from sailfish 3's full dataset. Video cameras were used to identify periods of conspecific interaction and ambient light, inset images across top panel. In the bottom panel depth is colour coded to % oxygen saturation from the animal-borne oxygen sensor, with the grey horizontal line representing the hypoxic boundary (60%–65% oxygen saturation).

remain for a short period, return to just above the hypoxic boundary for a short period where percent oxygen saturations were high, and then dive back down below the hypoxic boundary for another brief period (Figure 6). This behaviour was often performed one or more times before returning to the surface (Figure 6).

4 | DISCUSSION

Despite blue marlin and sailfish being ubiquitous in tropical and subtropical pelagic waters, and their economic and ecological importance, most information relating to their habitat use comes from course-scale satellite transmitting tags (Braun et al., 2015). As such, their fine-scale diving and foraging behaviour, and limits with regard to in situ water temperature and oxygen saturation have lagged behind other pelagic predators (e.g. sharks and tunas; but see Arostegui et al., 2022). This information is hindered by the challenges associated with direct observation of billfish behaviour due to their cryptic nature and inability to be maintained in captivity. Here, we combined a suite of biologging technologies to document the fine-scale habitat use of blue marlin and sailfish in the vertically compressed ETP. Further, we report on a previously undocumented behaviour that may be widespread among highly mobile marine predators, and an important component of their behaviour and foraging success.

We found substantial evidence of vertical habitat compression due to the sharp and simultaneous declines in both temperature and dissolved oxygen at shallow (~30–40 m) depths. Hypoxia and low temperatures are known to limit the horizontal and vertical distribution of istiophorid billfishes, with a synergistic effect when they act in concert (Carlisle et al., 2017; Prince et al., 2010). For example, blue marlin in the central Pacific made shallower dives in regions where both oxygen and temperature were limiting at depth, but less so when only one was limiting (Carlisle et al., 2017). Due to

cardiac temperature thresholds, istiophorid billfishes maximum diving depths are predicted to be limited by a temperature difference relative to the surface mixed layer of 8°C (ΔT 8°C), rather than absolute water temperature (Brill et al., 1993). Our results are consistent with this finding for both species, with a maximum ΔT of 7.8°C for sailfish and 8.5°C for blue marlin. While larger individuals are able to spend more time at deeper depths due to increased thermal inertia (Williams, Holmes, et al., 2017), this pattern was not observed here between blue marlin and sailfish likely due to the similarly shallow depths of both the thermocline and hypoxic boundary.

Contrary to temperature, absolute oxygen concentration should limit dive depth regardless of surface oxygen levels. Species that share similar physiology, gill morphology, and respiratory mode to istiophorid billfishes have been shown to experience physiological stress when dissolved oxygen (DO) decreases below $3.5\,mL\,L^{-1}$ (Bushnell & Brill, 1991; Wegner et al., 2010), which occurred at ~40 m during the study period. However, of the fish that dove past these depths, they did not remain there for extended periods, even during long duration dives. Marlin and sailfish often remained at or near the $3.5\,mL\,L^{-1}$ isopleth (38–40 m), and made periodic, brief forays below the isopleth (Figures 1, 2 and 6). While sustained activity at these oxygen levels is not possible, blue, black *Istiompax indica* and striped marlin *Kajikia audax* have been observed to make brief 'spike' dives to depths with DO $<3.5\,mL\,L^{-1}$ in the Eastern Tropical Atlantic and Indian Ocean, where oxygen minimum zones also exist near the surface (Prince et al., 2010; Rohner et al., 2022). These findings suggest that the $3.5\,mL\,L^{-1}$ boundary is not an absolute barrier to istiophorid vertical movements, but limits dive duration past the boundary (Prince et al., 2010; this study). It should be noted that Rohner et al. (2022) and Prince et al. (2010) used climatological modelled oxygen data, suggesting caution when interpreting oxygen levels actually experienced. Here, we confirm via animal-borne oxygen sensor measurements that tagged billfish move into water with ambient oxygen concentrations $<3.5\,mL\,L^{-1}$ for brief periods.

Motivations for diving in marine predators have been linked to several interacting factors, including energy conservation, behavioural thermoregulation, navigation and foraging (Carey et al., 1990; Gleiss et al., 2011; Klimley et al., 2002; Thompson et al., 1991). For example, by moving both horizontally and vertically, animals may reduce energy consumption while simultaneously increasing prey encounter rate without substantially increasing distance travelled (Andrzejaczek et al., 2020). Variable dive shapes, which have been observed in a wide range of pelagic predator taxa (Beck et al., 2003; Kerstetter et al., 2011; Seminoff et al., 2006) may also serve various purposes. V and U dives are among the most common and are thought to correspond to transiting and/or prey searching (V dives), or prey patch exploitation (i.e. foraging; U dives). However, U dives were the most common dive shape exhibited here for blue marlin and sailfish (51% and 34%, respectively), yet only one foraging attempt was caught on video during a W dive (see Logan et al., 2023). Therefore, rather than prey patch exploitation, we hypothesize that pelagic predators performing U dives (where dive depth is much shallower than bottom depth) are more likely searching for prey higher in the water column (i.e. looking for silhouettes) or searching along features that congregate prey (e.g. thermocline, pycnocline). Due to the high temporal resolution data obtained here, we identified additional dive shapes not yet reported for billfish, including W, LD and LA. LA dives were the second most common dive shape exhibited by sailfish (Table 2), suggesting sailfish often perform slow and shallow ascents, likely searching for prey in surface waters from below. Like U dives, W dives are proposed to be foraging dives in seabirds and pinnipeds (Bailleul et al., 2007; Halsey et al., 2007), and we provide evidence below of a similar function for billfish in the ETP.

The preferred prey of blue marlin and sailfish in the ETP (e.g. carangids, clupeids, scombrids) are subjected to the same vertical habitat restrictions as istiophorid billfish (Evans et al., 1981; Prince & Goodyear, 2006). Because many of these prey species are diel vertical migrators (Luo et al., 2000; Yasuda et al., 2018), and ram ventilation is limited by the upper margins of oxygen minimum zones (Bianchi et al., 2013), the abundance of these prey fish increases around this oxygen boundary during daylight hours (Bertrand et al., 2006; Bertrand et al., 2010). For example, in Pacific Nicaraguan waters, thread herring *Opisthonema libertate* biomass was found to be highest immediately above the 3–4 mL L^{-1} DO isopleth during daylight hours (Ehrhardt & Fitchett, 2006). For blue marlin and sailfish, path tortuosity was highest during U and W dives at depths near the thermocline and the 3–4 mL L^{-1} DO isopleth. Blue marlin path tortuosity was high at cold temperatures during U dives, and below the thermocline during W dives. Sailfish path tortuosity was also greatest during U and W dives and displayed a peak in tortuosity at a median depth of 39 m and median oxygen saturation of 65% (~3.4 mL L^{-1}), which are remarkably similar to the calculated hypoxic boundary (39.8 ± 2 m; 60%–65% O$_2$ saturation). Straight line movement is the most energetically efficient form of travel, and optimal search strategies should continue in straight lines unless the potential benefits of turning offset the cost (Wilson et al., 2013). Tortuous

movements are known to occur during prey searching behaviour and have been linked to increased foraging success in many marine animals (Adachi et al., 2017; Austin et al., 2006). As such, based on path tortuosity and physical characteristics of each dive type, we propose that V, LD, and LA dives (low tortuosity) were transiting and passive prey searching, while U and W dives (high tortuosity) were active prey searching and foraging dives near vertical habitat fronts with increased prey abundance.

The propensity for sailfish to repeatedly descend below the hypoxic boundary during the bottom phase of W dives suggests these descents are intentional (e.g. Figure 6). We propose this behaviour represents a foraging tactic where sailfish briefly dive below the hypoxic boundary (and by extension, below the prey) and search for prey silhouettes backlit by downwelling surface light. Istiophorid billfishes possess several adaptations supporting this hypothesis. For example, the marlin eye is acutely adapted for sensitivity at low light levels such as those experienced during deep foraging dives in the ETP (Figure 6; Fritsches, Marshall, et al., 2003). Similarly, high retinal cell density and the three visual pigments necessary for trichromatic colour vision are only present together in the ventral part of the eye, indicative of colour vision and high visual acuity in the visual field above and ahead of the animal (Fritsches, Litherland, et al., 2003). Furthermore, istiophorids possess a thermogenic organ beneath the brain, adjacent to the eyes that generates and maintains elevated temperatures relative to ambient (Block, 1986). During vertical movements into cold low-light waters, heating by this organ results in the maintenance of high speed of vision, and up to an order of magnitude greater temporal resolution of the eyes compared to their prey (Fritsches et al., 2005). Together, these features suggest that marlin and sailfish are specially adapted to hunt in cool, dark waters and ambushing prey from below. A conceptual framework for the evolution, maintenance, and importance of ambush predation in the pelagic environment supports this, suggesting that due to the lack of vertical structure to hide behind, many pelagic predators must attack from below (Bakun, 2022a, 2022b). Bluefin tuna have been observed to make frequent bounce dives through the thermocline during the day in highly stratified waters, suggested to be foraging dives (Kitagawa et al., 2000) but may be an example of the behaviour we describe here. Indeed, the only predation attempt caught on video during tag deployments began at the bottom a W dive of sailfish 6, where the pursuit was initiated at depth in cold, low oxygen, dimly-lit water (57 m; 22°C; 10%–20% O$_2$ saturation), featured a rapid ascent (reaching 3.1 ms^{-1}) and ended at the surface (see Logan et al., 2023).

5 | CONCLUSIONS

Here we have provided insights into predator diving and foraging behaviour along vertical fronts as well as how these predators respond to and use low oxygen environments. Given the limited spatial coverage of this study in relation to the large geographic range of these species, it is likely the behaviours exhibited here are not

characteristic to these species as a whole, and foraging strategies may be plastic depending on the environmental conditions experienced. However, we believe that new high-resolution biologging methods, such as those used here, will reveal the use of vertical fronts by marine predators is more widespread than currently represented in the literature. Further, the collective influence of climate change, global deoxygenation and shoaling oxygen minimum zones will reduce available habitat throughout the world's oceans and affect many marine organisms through direct and indirect pathways. Here, we suggest that the apex predators of the ETP are using the vertical fronts created by a hypoxic boundary layer to their advantage to increase foraging opportunities. Thus, predators currently unaffected by hypoxic boundary layers may be able to behaviorally adapt to spreading deoxygenation and the creation of shallow hypoxic boundary layers to maximize fitness. Because apex predators play important roles in structuring and regulating ecosystems, understanding how they will respond to and use low oxygen environments and the habitat fronts they create, as we have presented here, is needed so real-time management strategies are best equipped to respond to changing open-ocean ecosystems.

AUTHOR CONTRIBUTIONS

Ryan Logan designed the study with input from Jeremy Vaudo, Bradley Wetherbee and Mahmood Shivji. Ryan Logan led the methodology, data collection, data analysis, and drafting the original version of the manuscript. All authors contributed to revising the manuscript and approved the final draft.

ACKNOWLEDGEMENTS

CONFLICT OF INTEREST STATEMENT

We have no conflicts of interest to disclose.

DATA AVAILABILITY STATEMENT

Data available from the Dryad Digital Repository https://doi.org/10.5061/dryad.r7sqv9sj4 (Logan, 2023).

ORCID

Ryan K. Logan https://orcid.org/0000-0002-4714-5632

REFERENCES

Adachi, T., Costa, D. P., Robinson, P. W., Peterson, S. H., Yamamichi, M., Naito, Y., & Takahashi, A. (2017). Searching for prey in a three-dimensional environment: Hierarchical movements enhance foraging success in northern elephant seals. *Functional Ecology*, *31*, 361–369.

Andrzejaczek, S., Gleiss, A. C., Lear, K. O., Pattiaratchi, C., Chapple, T. K., & Meekan, M. G. (2020). Depth-dependent dive kinematics suggest cost-efficient foraging strategies by tiger sharks. *Royal Society Open Science*, *7*, 200789. https://doi.org/10.1098/rsos.200789

Andrzejaczek, S., Gleiss, A. C., Lear, K. O., Pattiaratchi, C. B., Chapple, T., & Meekan, M. (2019). Biologging tags reveal links between fine-scale horizontal and vertical movement behaviours in tiger sharks (*Galeocerdo cuvier*). *Frontiers in Marine Science*, *6*, 229.

Arostegui, M. C., Gaube, P., Woodworth-Jefcoats, P. A., Kobayashi, D. R., & Braun, C. D. (2022). Anticyclonic eddies aggregate pelagic predators in a subtropical gyre. *Nature*, *609*, 535–540.

Austin, D., Bowen, W. D., McMillan, J. I., & Iverson, S. J. (2006). Linking movement, diving, and habitat to foraging success in a large marine predator. *Ecology*, *87*, 3095–3108.

Bailleul, F., Charrassin, J.-B., Ezraty, R., Girard-Ardhuin, F., McMahon, C. R., Field, I. C., & Guinet, C. (2007). Southern elephant seals from Kerguelen Islands confronted by Antarctic Sea ice. Changes in movements and in diving behaviour. *Deep Sea Research Part II: Topical Studies in Oceanography*, *54*, 343–355. https://doi.org/10.1016/j.dsr2.2006.11.005

Bakun, A. (2022a). Adjusting intuitions as to the role of oxygen constraints in shaping the ecology and dynamics of ocean predator–prey systems. *Environmental Biology of Fishes*, *105*, 1287–1299.

Bakun, A. (2022b). Vertical ambush corridors: Intriguing multi-mechanism ecological structures embedded in the kinetic fluid architectures of ocean living resource production systems. *Fish and Fisheries*, *24*, 3–20.

Beck, C. A., Bowen, W. D., McMillan, J. I., & Iverson, S. J. (2003). Sex differences in the diving behaviour of a size-dimorphic capital breeder: The grey seal. *Animal Behaviour*, *66*, 777–789.

Bertrand, A., Ballon, M., & Chaigneau, A. (2010). Acoustic observation of living organisms reveals the upper limit of the oxygen minimum zone. *PLoS ONE*, *5*, e10330. https://doi.org/10.1371/journal.pone.0010330

Bertrand, A., Barbieri, M. A., Gerlotto, F., Leiva, F., & Córdova, J. (2006). Determinism and plasticity of fish schooling behaviour as exemplified by the South Pacific jack mackerel *Trachurus murphyi*. *Marine Ecology Progress Series*, *311*, 145–156.

Bianchi, D., Galbraith, E. D., Carozza, D. A., Mislan, K., & Stock, C. A. (2013). Intensification of open-ocean oxygen depletion by vertically migrating animals. *Nature Geoscience*, *6*, 545–548.

Block, B. A. (1986). Structure of the brain and eye heater tissue in marlins, sailfish, and spearfishes. *Journal of Morphology*, *190*, 169–189.

Braun, C. D., Arostegui, M. C., Thorrold, S. R., Papastamatiou, Y. P., Gaube, P., Fontes, J., & Afonso, P. (2022). The functional and ecological significance of deep diving by large marine predators. *Annual Review of Marine Science*, *14*, 129–159.

Braun, C. D., Kaplan, M. B., Horodysky, A. Z., & Llopiz, J. K. (2015). Satellite telemetry reveals physical processes driving billfish behavior. *Animal Biotelemetry*, *3*, 2. https://doi.org/10.1186/s40317-014-0020-9

Brill, R. W., Holts, D., Chang, R., Sullivan, S., Dewar, H., & Carey, F. (1993). Vertical and horizontal movements of striped marlin (*Tetrapturus audax*) near the Hawaiian islands, determined by ultrasonic telemetry, with simultaneous measurement of oceanic currents. *Marine Biology*, *117*, 567–574.

Brill, R. W., Lowe, T. E., & Cousins, K. L. (1998). How water temperature really limits the vertical movements of tunas and billfishes–it's the heart stupid. In K. Gamperl, D. MacKinlay, & A. Farrell (Eds.), *International congress on biology of fish* (p. 4). American Fisheries Society, Towson University.

Bushnell, P. G., & Brill, R. W. (1991). Responses of swimming skipjack (*Katsuwonus pelamis*) and yellowfin (*Thunnus albacares*) tunas to

acute hypoxia, and a model of their cardiorespiratory function. *Physiological Zoology*, *64*, 787–811.

Carey, F., Scharold, J., & Kalmijn, A. J. (1990). Movements of blue sharks (*Prionace glauca*) in depth and course. *Marine Biology*, *106*, 329–342.

Carlisle, A. B., Kochevar, R. E., Arostegui, M. C., Ganong, J. E., Castleton, M., Schratwieser, J., & Block, B. A. (2017). Influence of temperature and oxygen on the distribution of blue marlin (*Makaira nigricans*) in the Central Pacific. *Fisheries Oceanography*, *26*, 34–48.

Carter, M. I. D., Bennett, K. A., Embling, C. B., Hosegood, P. J., & Russell, D. J. (2016). Navigating uncertain waters: A critical review of inferring foraging behaviour from location and dive data in pinnipeds. *Movement Ecology*, *4*, 1–20.

Coffey, D. M., & Holland, K. N. (2015). First autonomous recording of in situ dissolved oxygen from free-ranging fish. *Animal Biotelemetry*, *3*, 47. https://doi.org/10.1186/s40317-015-0088-x

Derenbach, J., Astheimer, H., Hansen, H., & Leach, H. (1979). Vertical microscale distribution of phytoplankton in relation to the thermocline. *Marine Ecology Progress Series*, *1*, 187–193.

Ehrhardt, N. M., & Fitchett, M. D. (2006). On the seasonal dynamic characteristics of the sailfish, *Istiophorus platypterus*, in the eastern Pacific off Central America. *Bulletin of Marine Science*, *79*, 589–606.

Evans, R., McLain, D., & Bauer, R. (1981). Atlantic skipjack tuna: Influences of mean environmental conditions on their vulnerability to surface fishing gear. *Marine Fisheries Review*, *43*, 1–11.

Fiedler, P. C. (2010). Comparison of objective descriptions of the thermocline. *Limnology and Oceanography: Methods*, *8*, 313–325.

Fiedler, P. C., & Lavín, M. F. (2017). Oceanographic conditions of the eastern tropical Pacific. In P. Glynn, D. Manzello, & I. Enochs (Eds.), *Coral reefs of the eastern tropical Pacific* (pp. 59–83). Springer.

Fortune, S. M., Ferguson, S. H., Trites, A. W., Hudson, J. M., & Baumgartner, M. F. (2020). Bowhead whales use two foraging strategies in response to fine-scale differences in zooplankton vertical distribution. *Scientific Reports*, *10*, 1–18.

Fritsches, K., Litherland, L., Thomas, N., & Shand, J. (2003). Cone visual pigments and retinal mosaics in the striped marlin. *Journal of Fish Biology*, *63*, 1347–1351.

Fritsches, K. A., Brill, R. W., & Warrant, E. J. (2005). Warm eyes provide superior vision in swordfishes. *Current Biology*, *15*, 55–58.

Fritsches, K. A., Marshall, N. J., & Warrant, E. J. (2003). Retinal specializations in the blue marlin: Eyes designed for sensitivity to low light levels. *Marine and Freshwater Research*, *54*, 333–341.

Gallo, N., & Levin, L. (2016). Fish ecology and evolution in the world's oxygen minimum zones and implications of ocean deoxygenation. *Advances in Marine Biology*, *74*, 117–198. https://doi.org/10.1016/bs.amb.2016.04.001

Gleiss, A. C., Norman, B., & Wilson, R. P. (2011). Moved by that sinking feeling: Variable diving geometry underlies movement strategies in whale sharks. *Functional Ecology*, *25*, 595–607.

Halsey, L., Bost, C.-A., & Handrich, Y. (2007). A thorough and quantified method for classifying seabird diving behaviour. *Polar Biology*, *30*, 991–1004.

Kassambara, A., & Mundt, F. (2017). *Package 'factoextra'*. Extract and visualize the results of multivariate data analyses 76.

Keeling, R. F., Körtzinger, A., & Gruber, N. (2010). Ocean deoxygenation in a warming world. *Annual Review of Marine Science*, *2*, 199–229.

Kerstetter, D. W., Bayse, S. M., Fenton, J. L., & Graves, J. E. (2011). Sailfish habitat utilization and vertical movements in the southern Gulf of Mexico and Florida Straits. *Marine and Coastal Fisheries*, *3*, 353–365.

Kitagawa, T., Nakata, H., Kimura, S., Itoh, T., Tsuji, S., & Nitta, A. (2000). Effect of ambient temperature on the vertical distribution and movement of Pacific bluefin tuna *Thunnus thynnus orientalis*. *Marine Ecology Progress Series*, *206*, 251–260.

Klimley, P. A., Beavers, S. C., Curtis, T. H., & Jorgensen, S. J. (2002). Movements and swimming behavior of three species of sharks in

La Jolla Canyon, California. *Environmental Biology of Fishes*, *63*, 117–135. https://doi.org/10.1023/A:1014200301213

Laffoley, D., & Baxter, J. M. (2019). *Ocean deoxygenation: Everyone's problem—Causes, impacts, consequences and solutions.* Full report. IUCN.

Logan, R. K. (2023). Data from: Patrolling the border: Billfish exploit the hypoxic boundary created by the world's largest oxygen minimum zone. *Dryad Digital Repository*, https://doi.org/10.5061/dryad.r7sqv9sj4

Logan, R. K., Luongo, S. M., Vaudo, J. J., Wetherbee, B. M., & Shivji, M. S. (2023). Hunting behavior of a solitary sailfish *Istiophorus platypterus* and estimated energy gain after prey capture. *Scientific Reports*, *13*, 1484.

Logan, R. K., Vaudo, J. J., Lowe, C. G., Wetherbee, B. M., & Shivji, M. S. (2022). High-resolution post-release behaviour and recovery periods of two highly prized recreational sportfish: The blue marlin and sailfish. *ICES Journal of Marine Science*, *79*, 2055–2068.

Luo, J., Ortner, P. B., Forcucci, D., & Cummings, S. R. (2000). Diel vertical migration of zooplankton and mesopelagic fish in the Arabian Sea. *Deep Sea Research Part II: Topical Studies in Oceanography*, *47*, 1451–1473. https://doi.org/10.1016/S0967-0645(99)00150-2

McMahon, T. E., & Matter, W. J. (2006). Linking habitat selection, emigration and population dynamics of freshwater fishes: A synthesis of ideas and approaches. *Ecology of Freshwater Fish*, *15*(2), 200–210. https://doi.org/10.1111/j.1600-0633.2006.00130.x

Mysterud, A., & Ims, R. A. (1998). Functional responses in habitat use: Availability influences relative use in trade-off situations. *Ecology*, *79*, 1435–1441.

Pinheiro, J., & Bates, D. (2006). *Mixed-effects models in S and S-PLUS*. Springer Science & Business Media.

Prince, E. D., & Goodyear, C. P. (2006). Hypoxia-based habitat compression of tropical pelagic fishes. *Fisheries Oceanography*, *15*, 451–464.

Prince, E. D., Luo, J., Phillip Goodyear, C., Hoolihan, J. P., Snodgrass, D., Orbesen, E. S., Serafy, J. E., Ortiz, M., & Schirripa, M. J. (2010). Ocean scale hypoxia-based habitat compression of Atlantic istiophorid billfishes. *Fisheries Oceanography*, *19*, 448–462.

Pyke, G. H., Pulliam, H. R., & Charnov, E. L. (1977). Optimal foraging: A selective review of theory and tests. *The Quarterly Review of Biology*, *52*, 137–154.

Rohner, C. A., Bealey, R., Fulanda, B. M., Prebble, C. E., Williams, S. M., & Pierce, S. J. (2022). Vertical habitat use by black and striped marlin in the Western Indian Ocean. *Marine Ecology Progress Series*, *690*, 165–183.

Ropert-Coudert, Y., Kato, A., & Chiaradia, A. (2009). Impact of small-scale environmental perturbations on local marine food resources: A case study of a predator, the little penguin. *Proceedings of the Royal Society B: Biological Sciences*, *276*, 4105–4109.

Sakamoto, K. Q., Sato, K., Ishizuka, M., Watanuki, Y., Takahashi, A., Daunt, F., & Wanless, S. (2009). Can ethograms be automatically generated using body acceleration data from free-ranging birds? *PLoS ONE*, *4*, e5379. https://doi.org/10.1371/journal.pone.0005379

Schreer, J. F., Hines, R. J. O., & Kovacs, K. M. (1998). Classification of dive profiles: A comparison of statistical clustering techniques and unsupervised artifical neural networks. *Journal of Agricultural, Biological, and Environmental Statistics*, *3*(4), 383. https://doi.org/10.2307/1400572

Seibel, B. A. (2011). Critical oxygen levels and metabolic suppression in oceanic oxygen minimum zones. *Journal of Experimental Biology*, *214*, 326–336.

Seminoff, J. A., Jones, T. T., & Marshall, G. J. (2006). Underwater behaviour of green turtles monitored with video-time-depth recorders: what's missing from dive profiles? *Marine Ecology Progress Series*, *322*, 269–280.

Sequeira, A. M., Rodríguez, J., Eguíluz, V. M., Harcourt, R., Hindell, M., Sims, D. W., Duarte, C. M., Costa, D. P., Fernández-Gracia, J., & Ferreira, L. (2018). Convergence of marine megafauna movement

patterns in coastal and open oceans. *Proceedings of the National Academy of Sciences of the United States of America*, 115, 3072–3077. https://doi.org/10.1073/pnas.1716137115

Stephens, D. W., & Krebs, J. R. (1986). *Foraging theory*. Princeton University Press.

Stewart, J. D., Smith, T. T., Marshall, G., Abernathy, K., Fonseca-Ponce, I. A., Froman, N., & Stevens, G. M. (2019). Novel applications of animal-borne crittercams reveal thermocline feeding in two species of manta ray. *Marine Ecology Progress Series*, 632, 145–158.

Stramma, L., Prince, E. D., Schmidtko, S., Luo, J., Hoolihan, J. P., Visbeck, M., Wallace, D. W., Brandt, P., & Körtzinger, A. (2012). Expansion of oxygen minimum zones may reduce available habitat for tropical pelagic fishes. *Nature Climate Change*, 2, 33–37.

Thompson, D., Hammond, P., Nicholas, K., & Fedak, M. A. (1991). Movements, diving and foraging behaviour of grey seals (*Halichoerus grypus*). *Journal of Zoology*, 224, 223–232.

Tibshirani, R., Walther, G., & Hastie, T. (2001). Estimating the number of clusters in a data set via the gap statistic. *Journal of the Royal Statistical Society, Series B: Statistical Methodology*, 63, 411–423.

Watanabe, Y. Y., & Takahashi, A. (2013). Linking animal-borne video to accelerometers reveals prey capture variability. *Proceedings of the National Academy of Sciences of the United States of America*, 110, 2199–2204.

Wegner, N. C., Sepulveda, C. A., Bull, K. B., & Graham, J. B. (2010). Gill morphometrics in relation to gas transfer and ram ventilation in high-energy demand teleosts: Scombrids and billfishes. *Journal of Morphology*, 271, 36–49.

Williams, H. J., Holton, M. D., Shepard, E. L., Largey, N., Norman, B., Ryan, P. G., Duriez, O., Scantlebury, M., Quintana, F., & Magowan, E. A. (2017). Identification of animal movement patterns using tri-axial magnetometry. *Movement Ecology*, 5, 6. https://doi.org/10.1186/s40462-017-0097-x

Williams, S. M., Holmes, B. J., Tracey, S. R., Pepperell, J. G., Domeier, M. L., & Bennett, M. B. (2017). Environmental influences and ontogenetic differences in vertical habitat use of black marlin (*Istiompax indica*) in the southwestern Pacific. *Royal Society Open Science*, 4, 170694.

Wilson, R., Griffiths, I., Legg, P., Friswell, M., Bidder, O., Halsey, L., Lambertucci, S. A., & Shepard, E. (2013). Turn costs change the value of animal search paths. *Ecology Letters*, 16, 1145–1150.

Wilson, R. P., Shepard, E., & Liebsch, N. (2008). Prying into the intimate details of animal lives: Use of a daily diary on animals. *Endangered Species Research*, 4, 123–137.

Wilson, R. P., White, C. R., Quintana, F., Halsey, L. G., Liebsch, N., Martin, G. R., & Butler, P. J. (2006). Moving towards acceleration for estimates of activity-specific metabolic rate in free-living animals: The case of the cormorant. *Journal of Animal Ecology*, 75, 1081–1090.

Wood, S. (2015). *Package 'mgcv'*. R Package Version 1:29.

Woodson, C. B., & Litvin, S. Y. (2015). Ocean fronts drive marine fishery production and biogeochemical cycling. *Proceedings of the National Academy of Sciences of the United States of America*, 112, 1710–1715.

Yasuda, T., Nagano, N., & Kitano, H. (2018). Diel vertical migration of chub mackerel: Preliminary evidence from a biologging study. *Marine Ecology Progress Series*, 598, 147–151.

Yoda, K., Sato, K., Niizuma, Y., Kurita, M., Bost, C., Le Maho, Y., & Naito, Y. (1999). Precise monitoring of porpoising behaviour of Adélie penguins determined using acceleration data loggers. *Journal of Experimental Biology*, 202, 3121–3126. https://doi.org/10.1242/jeb.202.22.3121

Zuur, A., Ieno, E., Walker, N., Saveliev, A., & Smith, G. (2009). *Mixed effects models and extensions in ecology with R*. Springer.

SUPPORTING INFORMATION

Additional supporting information can be found online in the Supporting Information section at the end of this article.

Table S1: *p*-values of pairwise comparisons of path tortuosity among blue marlin dive shapes from non-parametric Games-Howell post-hoc test.

Table S2: *p*-values of pairwise comparisons of path tortuosity among sailfish dive shapes from non-parametric Games-Howell post-hoc test.

Table S3: Blue marlin tortuosity GAMM results.

Table S4: Sailfish tortuosity GAMM results.

Figure S1: Detailed view of the custom biologging tag package built to quantify blue marlin and sailfish fine scale behavior and habitat use with and without an oxygen sensor.

Figure S2: Various methods used to determine the optimal number of dive shapes (i.e., clusters) for blue marlin (top) and sailfish (bottom).

Figure S3: Screen shots from video footage of sailfish 6.

Video S1

Video S2